Int J Adv Manuf Technol (2017) 92:259–275
DOI 10.1007/s00170-017-0086-7

ORIGINAL ARTICLE

Multi-variable driving thermal energy control model of dry hobbing machine tool

Libin Zhu[1] · **Huajun Cao**[1] · **Dan Zeng**[1] · **Xiao Yang**[1] · **Benjie Li**[1]

Received: 19 November 2016 / Accepted: 16 January 2017 / Published online: 22 February 2017

Abstract Dry hobbing is a new gear machining process with high efficiency and environmental friendliness, replacing traditional wet hobbing process. However, to get high reliable precision, it is a critical work for the dry hobbing system to reduce and control the thermal impact. Even new hobbing machine tool structure with high thermal stability such as double stand columns was designed to substitute the traditional structure; some new structures, such as air extraction and filtration device, air-cooling component, and magnetic chip conveyor, would affect the thermal energy accumulation of dry hobbing machine tool. In this paper, a multi-variable thermal energy control model was developed to describe the thermal energy accumulation characteristic of dry hobbing machine tool. Variables which would affect thermal energy generation and sink of dry hobbing machine tool are analyzed. A multi-objective optimization algorithm is proposed for variable optimization, combined with the multi-variable thermal energy control model. An application method is presented to show the thermal energy control procedure of dry hobbing machine tool. As a result, the temperature variation of interior space air, workpiece column, and anterior end cover is fluctuated in an acceptable range with optimization. Furthermore, thermal deformation errors, which range from −7 to 3 μm, could meet production requirements. It illustrates that the multi-variable driving thermal energy control model of dry hobbing machine tool is available.

Keywords Dry hobbing machine tool · Thermal energy control model · Thermal energy accumulation · Multi-variable optimization

✉ Huajun Cao
hjcao@cqu.edu.cn

[1] State Key Laboratory of Mechanical Transmission, Chongqing University, Chongqing 400044, China

1 Introduction

Gear hobbing is the leading manufacturing technology for mass production of gears, especially for automobile gears. However, the widely used wet gear hobbing process, which consumes lots of metalworking fluids, leads to environmental pollution and healthy risk of workers. In recent years, dry hobbing becomes available. And it would replace wet hobbing in the coming future quickly, due to its high efficiency and environmental friendliness. According to Bryan [1], thermal errors, which make up 40–70% of the total machine tool errors, are the greatest contributors to machine tool errors. Significant research has been done on thermal behavior and thermal errors of machine tool. Holkup et al. [2] presents a finite-element-method-based thermomechanical model of spindles with rolling bearings. Kim et al. [3] investigated important heat sources and resulting thermal errors in a machine tool equipped with linear motors when the machine tool was operated at high speed. Huang et al. [4] presents a novel method for measuring real-time temperature field of a heavy-duty machine tool.

Nevertheless, few researchers focused on modeling and control of thermal energy accumulation of hobbing machine tool as a system. In traditional wet hobbing, the implementation of flood metalworking fluids in machining process reduces the generation of frictional heat and makes the temperature of chips, hob, and workpiece close to metalworking fluids' temperature, the variation of which is little, by convective cooling. Thus, researches about machine tool thermal models are mainly focused on machine tool spindle units [5–8], which are the main components whose temperature is relatively high and needs to be controlled. Generally, the modeling method of spindle units is based on motor efficiency and heat transfer [9, 10]. According to Sreejith and Ngoi [11], there are more friction and adhesion between the hob and the workpiece in dry hobbing, since they will be subjected to higher temperatures. And without

metalworking fluids, the cutting heat makes the temperature of chips, hob, and workpiece relatively high [12], which would lead to thermal energy accumulation and temperature rise of machine tool components. In order to reduce and control the thermal impact of dry hobbing, new hobbing machine tool structure with high thermal stability such as double stand columns was designed to substitute the traditional structure. However, in dry hobbing, the worse cooling condition [13] makes the machine tool components' temperature sensitive to relevant parameters and ambient temperature. Furthermore, some new structures, such as air extraction and filtration device, air-cooling component, and magnetic chip conveyor, would affect the thermal energy accumulation of dry hobbing machine tool. Without a thermal energy control model, which is used to calculate the value of thermal energy accumulation and optimize relevant parameters, it is hard to make the temperature of dry hobbing machine tool components constant, which would lead to bad machining precision [14–16], decrease of hob life, etc. [17, 18]. Thus, a thermal energy control model of dry hobbing machine tool is needed to optimize relevant parameters and make the temperature variation of machine tool components fluctuate in an acceptable range.

This paper proposes a multi-variable thermal energy control model of dry hobbing machine tool, which is based on the first law of thermodynamics. The thermal energy generation and sink of dry hobbing machine tool, as well as effect of air extraction and filtration device, air-cooling component, and magnetic chip conveyor, are analyzed. The relevant parameters, which would affect the thermal energy accumulation of dry hobbing machine tool, are presented. With this model, the thermal energy change of dry hobbing machine tool over a time interval could be calculated. An application method, which incorporates the multi-variable driving thermal energy control model and the multi-objective optimization algorithm, is presented to show the procedure of thermal energy control of dry hobbing machine tool. With application, temperature variation of interior space air, workpiece column, and anterior end cover is fluctuated in an acceptable range. Furthermore, thermal deformation errors of the dry hobbing machine tool is presented to evaluate whether the optimization could meet production requirements. The result shows that the multi-variable thermal energy control model of dry hobbing machine tool is effective.

2 Preliminary study

In this paper, a kind of dry hobbing machine tool is taken as the research object. The method that is proposed in this paper is suitable for other kinds of dry hobbing machine tool generally.

In wet hobbing, implementation of flood metalworking fluids, whose mass flow rate and specific heat capacity are relative high, reduces the generation of frictional heat in machining process and decreases temperature by convective cooling. The temperature of chips, workpiece, and hob is close to the temperature of metalworking fluids, the variation of which is small. The cutting heat that transfers to other machine tool components is too little to cause the temperature rise.

In dry hobbing, the cutting heat is mainly taken away from dry hobbing machine tool by compressed cold air and chips. Compressed cold air is used to cool the cutting zone and benefit chip removing. Due to the low specific heat capacity of compressed cold air, the temperature of chips, workpiece, and hob is higher than in wet hobbing. The thermal energy that accumulated in chips, workpiece, and hob will transfer into interior space air, hob holder, workpiece holder, machine tool bed, etc. The temperature of compressed cold air will rise after it passes through the cutting zone. As dry hobbing machine tool is not well ventilated, the high-temperature air exchanges heat with other components whose temperature is relative low. Heat exchange in dry hobbing machine tool is slow and complex. The characters of dry hobbing compared with ordinary wet hobbing are mainly:

1. When compressed cold air is used instead of metalworking fluids, the cooling effect is much less pronounced than that of metalworking fluids. The worse cooling condition makes temperature of chips, workpiece, and hob higher than in wet hobbing.
2. Some of the thermal energy that is stored in chips, interior space air, hob, and workpiece will transfer to other machine tool parts. Heat exchange in dry hobbing machine tool is slow and complex.
3. In dry hobbing, the temperature of chips is much more higher than ambient temperature commonly. Thus, the thermal energy of chips will transfer to the interior space air.

As dry hobbing machine tool eliminates the using of metalworking fluids, the structure of dry hobbing machine tool is different from ordinary wet hobbing machine tool. Some new structures, such as air extraction and filtration device, air-cooling component, and magnetic chip conveyor, that are used in dry hobbing machine tool, would affect the thermal energy accumulation of dry hobbing machine tool. The machine tool bed is designed with inclined surface to make sure that the chips could fall on the magnetic chip conveyor below the machine tool bed, as shown in Fig. 1. Air extraction and filtration device, which is used for dust filtering, could also affect the airflow between ambient and interior space of dry hobbing machine tool.

For a dry hobbing machine tool system, the main components, which are placed out of the machine tool, are commonly electric control cabinet, motor coolant station, part of the chip conveyor, chip container, lubricating station, pneumatic

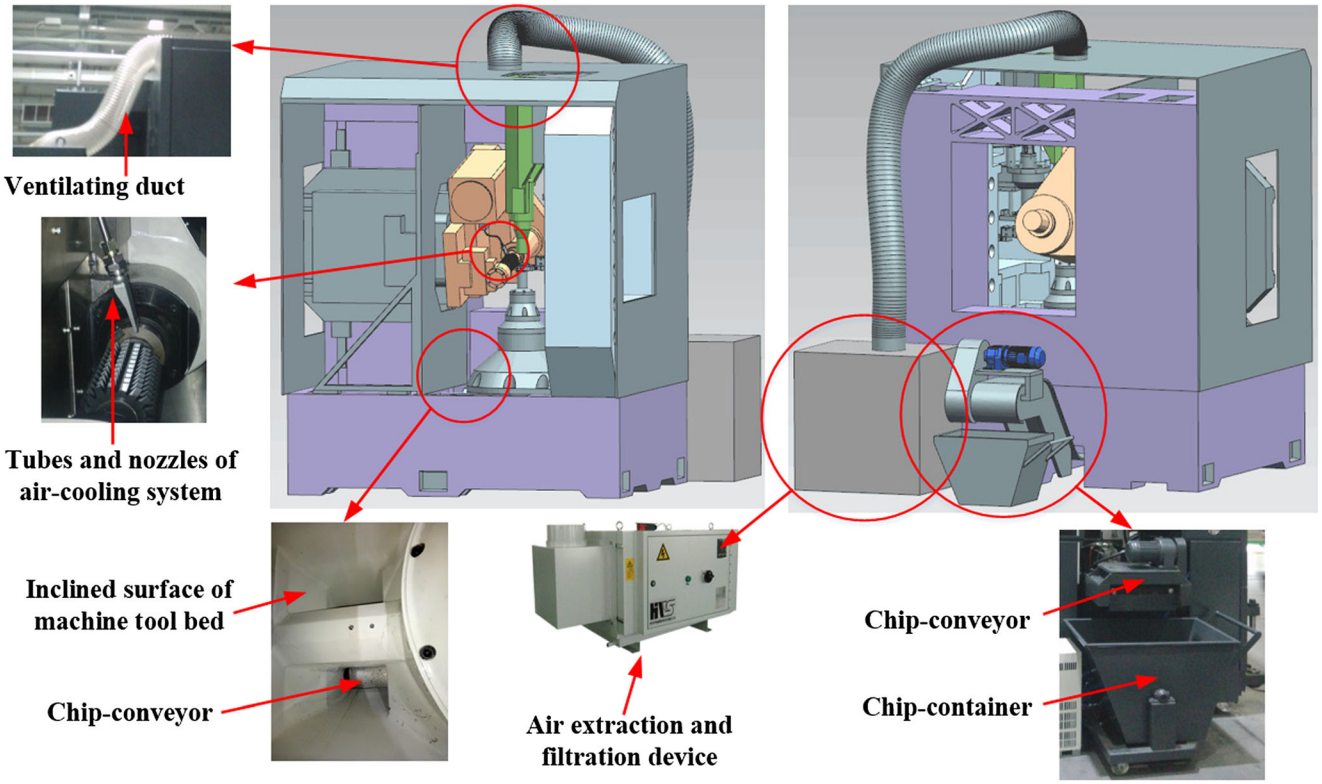

Fig. 1 New structures of dry hobbing machine tool (front view and back view)

station, hydraulic station, automatic feeding component, and CNC panel, as shown in Fig. 2. In the electric control cabinet are mainly control system and high-voltage electronic parts. As there is a temperature control device in the electric control cabinet, and it is out of touch with the dry hobbing machine tool, the thermal energy that is generated in it would not conduct to the dry hobbing machine tool. The motor coolant station is mainly used for motor cooling. During process, chips are falling on the chip conveyor, that blows the cutting zone, and removed from machine tool to the chip container. The

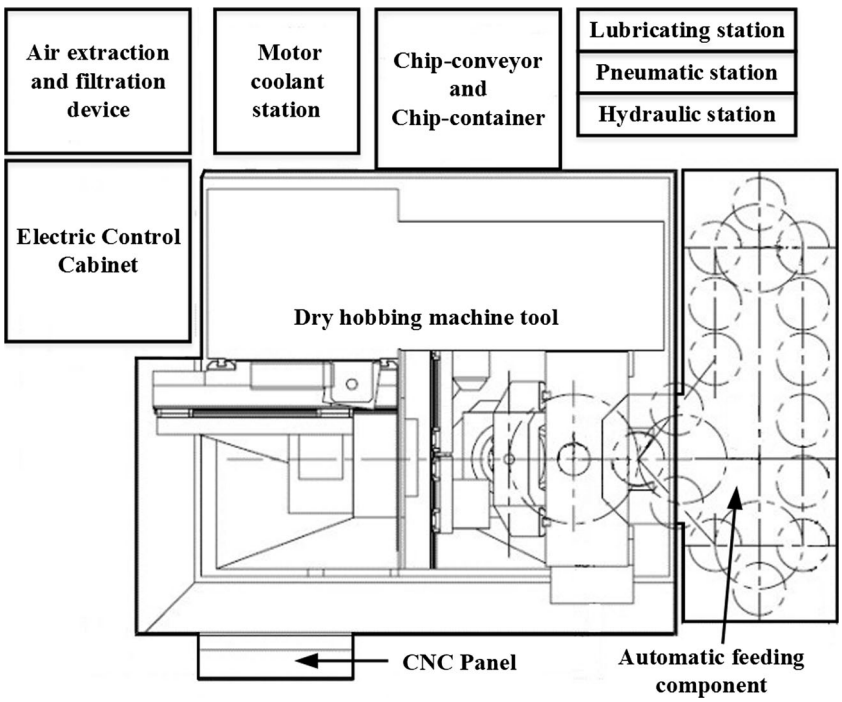

Fig. 2 Sketch of components of dry hobbing machine tool system (top view)

lubricating station is mainly composed of a lubricating oil container, filter, lubricating grease pump, motor, etc. The hydraulic station is mainly composed of a hydraulic oil container, filter, hydraulic pump, solenoid valve, motor, etc. The automatic feeding component, which is close to the manipulator, is used to load and unload workpiece. The pneumatic station could dry and cool the compressed air, which is supplied by a workshop compressed air station. As components that are mentioned above are out of touch with dry hobbing machine tool, thermal energy change of them would not affect the dry hobbing machine tool. Thus, it is the dry hobbing machine tool except for the above components, which are shown in Fig. 2, that was analyzed as an open thermodynamic system.

3 Multi-variable driving thermal energy control model

According to the first law of thermodynamics, over a time interval [19], the amount of energy increase of a machine tool is equal the amount of energy that enters the machine tool, minus the amount of energy that leaves the machine tool. The total energy, E, is consist of kinetic energy, E_k, gravitational potential energy, E_p, and internal energy, U. And the internal energy is consist of sensible energy, latent energy, chemical energy, and nuclear energy. For dry hobbing machine tool, the main part that leads to temperature variation is sensible energy, which refers to thermal energy. Hence, for dry hobbing machine tool, it follows that

$$\Delta E = \Delta E_k + \Delta E_p + \Delta U \tag{1}$$

where ΔE is the total energy change of dry hobbing machine tool, ΔE_k is the kinetic energy change of dry hobbing machine tool, ΔE_p is the gravitational potential energy change of dry hobbing machine tool, and ΔU is the internal energy change, i.e., thermal energy change of dry hobbing machine tool.

The energy that is supplied to dry hobbing machine tool is mainly converted to thermal energy and strain energy at last. In dry hobbing, the main heat generation is caused by cutting work and movements of machine tool parts, which are driven by motors. Thus, the electrical energy that is supplied to dry hobbing machine tool motors is considered as the energy input of dry hobbing machine tool. Electrical energy that is supplied to other electrical parts such as electronic control parts and lighting parts is neglected. The thermal energy sink of dry hobbing machine tool is mainly caused by chip removal, workpiece removal, airflow, lubricating oil convection, motor coolant convection, hydraulic oil convection, convection between dry hobbing machine tool and ambient, radiation, etc. Thus, Eq. (2) can be obtained.

$$\begin{aligned} &E_T - \Delta E_L - \Delta E_{Mc} - \Delta E_H - \Delta E_A - \Delta E_C - E_R - \Delta E_{Wp} - \Delta E_{Ch} \\ &\quad = \Delta E_k + \Delta E_p + \Delta U \end{aligned} \tag{2}$$

where E_T is the thermal energy that is generated in dry hobbing machine tool, ΔE_L is the thermal energy of dry hobbing machine tool which transfers into lubricant by convection, ΔE_{Mc} is the thermal energy of dry hobbing machine tool which transfers into motor coolant by convection, ΔE_H is the thermal energy of dry hobbing machine tool which transfers into hydraulic oil by convection, ΔE_A is the thermal energy change of dry hobbing machine tool that is caused by airflow, E_C is the thermal energy that outflows by convection between dry hobbing machine tool surface and ambient, E_R is thermal energy that outflows by radiation, ΔE_{Wp} is the thermal energy increment of processed workpieces when they are removed out of the dry hobbing machine tool, and ΔE_{Ch} is the thermal energy increment of chips when they are removed out of the dry hobbing machine tool.

Dry hobbing machine tool needs to be adjusted after test hobbing. Then, the spindles need to be warmed up before process. Thus, the time point that the spindles are warmed up should be the starting point of thermal energy accumulation of dry hobbing machine tool. The thermal energy generation and sink of dry hobbing machine tool are shown in Fig. 3.

3.1 Electrical energy supplied to motors

The main movements of dry hobbing machine tool components, which are driven by motors, are the following:

1. Rotation of hob, which is shown as B in Fig. 4
2. Radial feed movement of tool post, which is shown as X in Fig. 4
3. Axial feed movement of tool post, which is shown as Z in Fig. 4
4. Tangential feed movement of tool post, that is, shifting of hob, which is shown as Y in Fig. 4
5. Rotation of tool post, which is shown as A in Fig. 4
6. Rotation of worktable, which is shown as C in Fig. 4
7. Axial feed movement of workpiece holder, which is shown as Z2 in Fig. 4

During processing, the angle of hob is remained unchanged in general. And the tangential feed movement only happens when hob shifting is needed. Thus, the process is going with other five movements mainly, that is, rotation of hob, radial feed movement of tool post, axial feed movement of tool post, tangential feed movement of tool post, and rotation of worktable. The electrical energy that is supplied to the corresponding five dry hobbing machine tool motors, E_M, is produced by

$$E_M = \sum_{i=1}^{5} \int_0^t P_i dt \tag{3}$$

where t is the time interval from the time point that the spindles are warmed up to the time point that is picked at the time

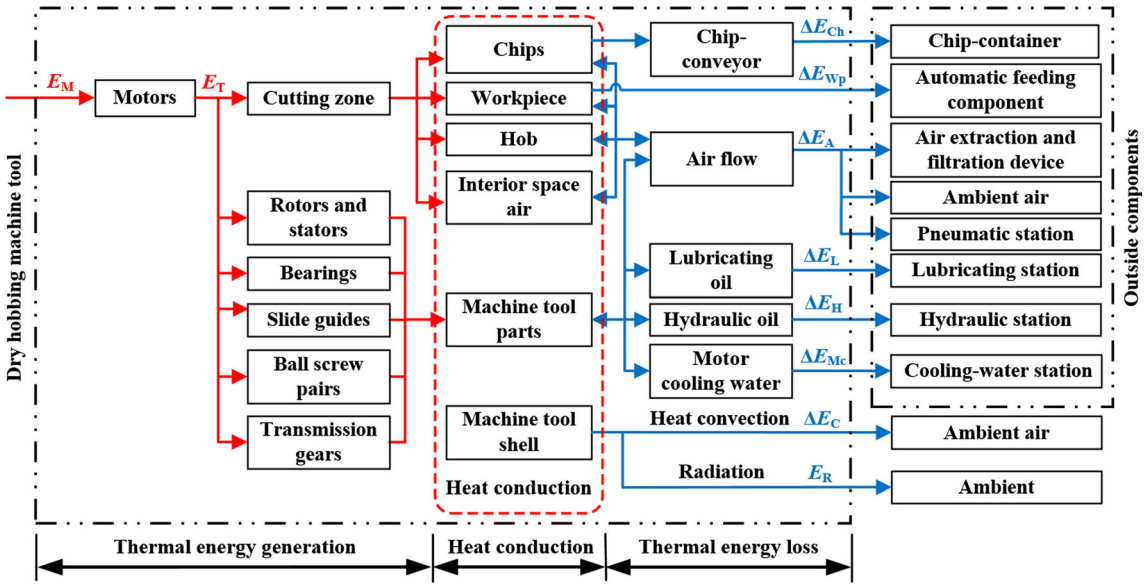

Fig. 3 Thermal energy generation and sink of dry hobbing machine tool

when the hob and workpiece are still and P_i ($i = 1, 2, 3, 4, 5$) is the supplied electrical power of corresponding motors.

The electrical energy that is supplied to dry hobbing machine tool motors is converted to kinetic energy that is used for cutting work and thermal energy that is generated in rotors, stators, bearings, guides, ball screw pairs, and transmission gears. It is a widely used assumption that almost all the energy required for machining is converted to thermal energy in the deformation zones and at the tool–chip interface while some studies showed that 85–95% of the total work is converted to thermal energy [20]. The other is converted to latent energy and kinetic energy of chips. Thus, when the workpiece and process parameters are keep unchanged, the thermal energy that is generated in dry hobbing machine tool, E_T, could be expressed as a constant coefficient, η, of E_M, that is,

$$E_T = \eta E_M = \eta \sum_{i=1}^{5} \int_0^t P_i dt \tag{4}$$

When the workpiece and process parameters are keep unchanged, η could be gained with an experiment that the value of E_M and E_T is measured and calculated. The thermal energy that is generated in the cutting zone could be gained by using a water-based calorimeter [21]. The method that is proposed by Chen et al. [22] could be used to calculate the thermal energy that is generated in motors. The method that is proposed by Kauschinger and Schroeder [23] could be used to calculate the thermal energy that is generated in bearings. The thermal energy that is generated in ball screw pairs could be gained by using the method that is proposed by Shi et al. [24]. The thermal energy that is generated by slide guide motion and gear transmission is mainly caused by friction [25]. Thus, E_T and E_M could be gained with the above method in the experiment. Then, η could be calculated with Eq. (4).

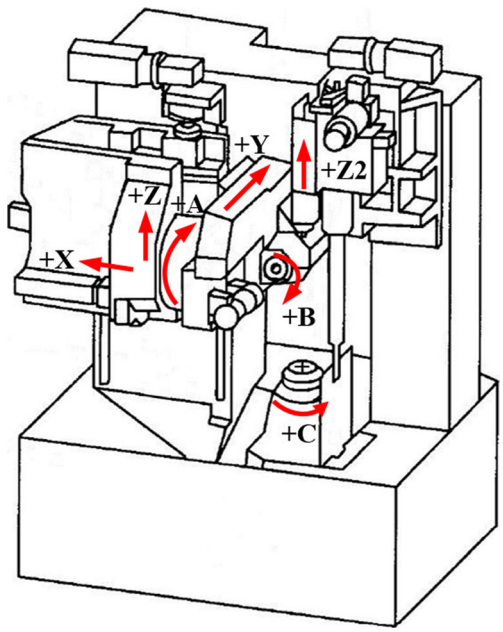

Fig. 4 Main movement of dry hobbing machine tool components

3.2 Thermal energy change caused by removing of workpieces

As there is no metalworking fluids in dry hobbing, the temperature of chips and processed workpiece is higher than that in wet hobbing. Some thermal energy is accumulated in processed workpiece and chips, which will be removed out of the dry hobbing machine tool. Figure 5 shows the thermography of processed workpiece; the temperature variation of points on the same cylinder of hobbed workpiece is less than 0.7 °C. It demonstrates that the temperature of hobbed workpiece is

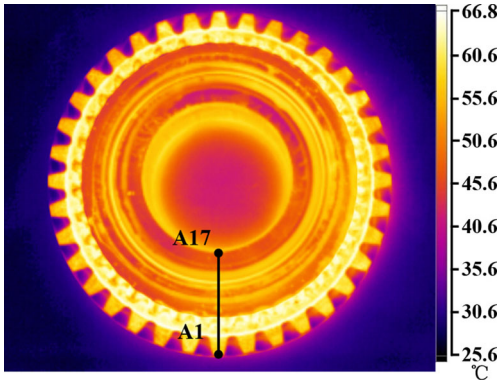

Fig. 5 Thermography of processed workpiece

approximately symmetric. Table 1 shows the temperature of points from A1 to A17, the maximum difference of which is 1.6 °C. Thus, the temperature field of processed workpiece can be simplified to even steady-state temperature field, in order to simplify the thermal model. The average value of those 17 points is defined as the value of workpiece temperature in this paper.

The thermal energy lost which is caused by removing of processed workpiece, ΔE_{Wp}, that is, thermal energy increment of processed workpieces when they are removed out of the machine tool, is produced by

$$\Delta E_{\mathrm{Wp}} = \sum_{j=1}^{n_1} c_{\mathrm{wp}} m_{\mathrm{wp}} \left(T_{\mathrm{wp2},j} - T_{\mathrm{wp1},j}\right) \tag{5}$$

where n_1 is the number of processed workpiece, c_{wp} is the specific heat capacity of workpiece, m_{wp} is the mass of one processed workpiece, $T_{\mathrm{wp1},j}$ is the temperature of the jth workpiece when it is moved in dry hobbing machine tool, and $T_{\mathrm{wp2},j}$ is the temperature of the jth workpiece when it is removed out of machine tool.

3.3 Thermal energy change caused by removing of chips

During hobbing, chips are falling on the chip conveyor and removed out of the machine tool. The kinetic energy and potential energy of chips are converted to thermal energy due to windage and collision. Potential energy change of chips is produced by

$$\Delta E_{\mathrm{p,ch}} = n_1 m_{\mathrm{ch}} g z \tag{6}$$

where m_{ch} is the mass of chips that move out from one workpiece and z is the altitude variation value of chips.

According to the thermography of chips, the temperature of chips from one workpiece when they are removed out of the machine tool fluctuates in a small range. Thus, in order to simplify calculation, the average temperature could be used in Eq. (7). And the thermal energy lost which is caused by removing of chips, ΔE_{Ch}, is produced by

$$\Delta E_{\mathrm{Ch}} = \sum_{j=1}^{n_1} c_{\mathrm{ch}} m_{\mathrm{ch}} \left(T_{\mathrm{ch2},j} - T_{\mathrm{wp1},j}\right) \tag{7}$$

where c_{ch} is the specific heat capacity of chips and $T_{\mathrm{ch2},j}$ is the average temperature of chips from the jth workpiece when they are removed out of the machine tool.

Equation (7) provides a method to calculate the thermal energy lost which is caused by removing of chips. Before chips are removed out of the dry hobbing machine tool, part of thermal energy of chips is conducted to interior space air. Changing corresponding parameters will affect the amount of thermal energy of chips which is conducted to interior space air and cause the variation of ΔE_{Ch}. For a chip, the Reynolds number, Re_L, which is used to determine the appropriate convection correlation for computing average Nusselt number, $\overline{\mathrm{Nu}}_L$, is determined as

$$Re_L = \frac{u_{\mathrm{cc}} L_{\mathrm{ch}}}{v} \tag{8}$$

where u_{cc} is the velocity of chip on chip conveyor which could be regarded as the velocity of airflow over chip, v is the kinematic viscosity of air around the chip conveyor, and L_{ch} is the characteristic length of chip.

As the flow is laminar over the entire chip, the average Nusselt number is given by

$$\overline{\mathrm{Nu}}_L = 0.664 {Re_L}^{1/2} \mathrm{Pr}^{1/3} \tag{9}$$

The average heat convection coefficient (W/(m^2 °C)) for the entire chip surface, $\overline{h}$, is defined as

$$\overline{h} = \frac{\overline{\mathrm{Nu}}_L k}{L_{\mathrm{ch}}} \tag{10}$$

Thus, for a chip, the heat transfer rate can be expressed as

$$q_{\mathrm{ch}} = \overline{h} A_{\mathrm{ch}} (T_{\mathrm{ch}} - T_{\mathrm{ia}}) = \frac{0.664 k {u_{\mathrm{cc}}}^{1/2} \mathrm{Pr}^{1/3} A_{\mathrm{ch}} (T_{\mathrm{ch}} - T_{\mathrm{ia}})}{v^{1/2} L^{1/2}} \tag{11}$$

where A_{ch} is the surface area of chip, T_{ch} is the temperature of chip, and T_{ia} is the temperature of interior space air that is close

Table 1 Temperature of points on hobbed workpiece

Number of points	A1	A2	A3	A4	A5	A6	A7	A8	A9
Temperature (°C)	61.1	61.3	61.0	61.1	61.4	61.7	61.5	61.1	60.7
Number of points	A10	A11	A12	A13	A14	A15	A16	A17	
Temperature (°C)	60.4	60.6	60.7	60.5	60.3	60.4	60.1	60.2	

to the chip. The interior space air which is far from the cutting zone could be seemed as quiescent with the same temperature.

Chen et al. [26] reveals the geometry behavior in cylindrical gear hobbing with mathematical model, as shown in Fig. 6, which leads to the conclusion that mathematical geometric configuration of undeformed chips could be divided into specific kinds. Moreover, CAD-based simulation of the hobbing process [27] provides the whole geometrical information of chips. Thus, for continuous processing, whose cutting parameters remain unchanged, the kinds and quantity of chips from different workpiece are regarded as the same. And the chips' geometry of prescribed kind could be regarded as the same, too. For chips from one workpiece, the heat that transfers to interior space air could be calculated as

$$Q_{\mathrm{Ch}} = \sum_r \sum_p \int_0^{t_{\mathrm{ch}}} \overline{h}_r A_{\mathrm{ch},r,p} (T_{\mathrm{ch}} - T_{\mathrm{ia}}) dt$$

$$= \sum_r \sum_p \int_0^{t_{\mathrm{ch}}} \frac{0.664 k {u_{\mathrm{cc}}}^{1/2} \mathrm{Pr}^{1/3} A_{\mathrm{ch},r,p} (T_{\mathrm{ch}} - T_{\mathrm{ia}})}{\nu^{1/2} L^{1/2}} dt \qquad (12)$$

where p is the number of cutting tooth, r is the repeated cutting times of pth cutting tooth, and t_{ch} is the time required for a chip to be removed out of the dry hobbing machine tool by the chip conveyor, and

$$t_{\mathrm{ch}} = \frac{L_{\mathrm{cc}}}{u_{\mathrm{cc}}} \qquad (13)$$

where L_{cc} is the chip moving length on the part of the chip conveyor which is under the dry hobbing machine tool bed, as shown in Fig. 7.

Since there is no change in Re_L or Pr associated with a change in T_{ch}, for constant properties, the local Nusselt number is unchanged. Moreover, since L and k are also unchanged, the local convection coefficient remains the same. Thus, Eq. (12) could be expressed as

$$Q_{\mathrm{Ch}} = f(u_{\mathrm{cc}}, t_{\mathrm{ch}}, T_{\mathrm{ch}}, T_{\mathrm{ia}}) \qquad (14)$$

When u_{cc} is a certain value, the value of Q_{Ch} could be gained by using a water-based calorimeter [21]. Thus, Q_{Ch} could be gained with the experimental value and Eq. (14).

3.4 Thermal energy change caused by airflow

In dry hobbing machine tool, compressed cold air is used instead of metalworking fluids. Air extraction and filtration device, which is used for dust filtering, could also affect the airflow between ambient and interior space of dry hobbing machine tool. As shown in Fig. 8, airflow in dry hobbing machine tool is mainly:

1. Compressed cold air that is supplied by the air-cooling component
2. Airflow between interior space and ambient that is caused by compressed cold air supply and air extraction

Air-cooling component is composed of compressed air source, refrigerated air dryer, control parts, tubes, nozzles, etc. The compressed air enters the refrigerated air dryer and be refrigerated. Then, the compressed cold air is separated into some parts to enter the dry hobbing machine tool:

1. One part of compressed air is used for the pneumatic door control component. As this part of compressed air is little, and the state of machine tool door is changed only when the processing is finished, the thermal energy change of dry hobbing machine tool that is caused by this part could be neglected.
2. Other n_2 parts of compressed cold air is used for cooling and chip removal.

The compressed cold air, which goes through tubes and nozzles to cool the cutting process, advantages cooling and chip removal. In dry hobbing machine tool, there are at least

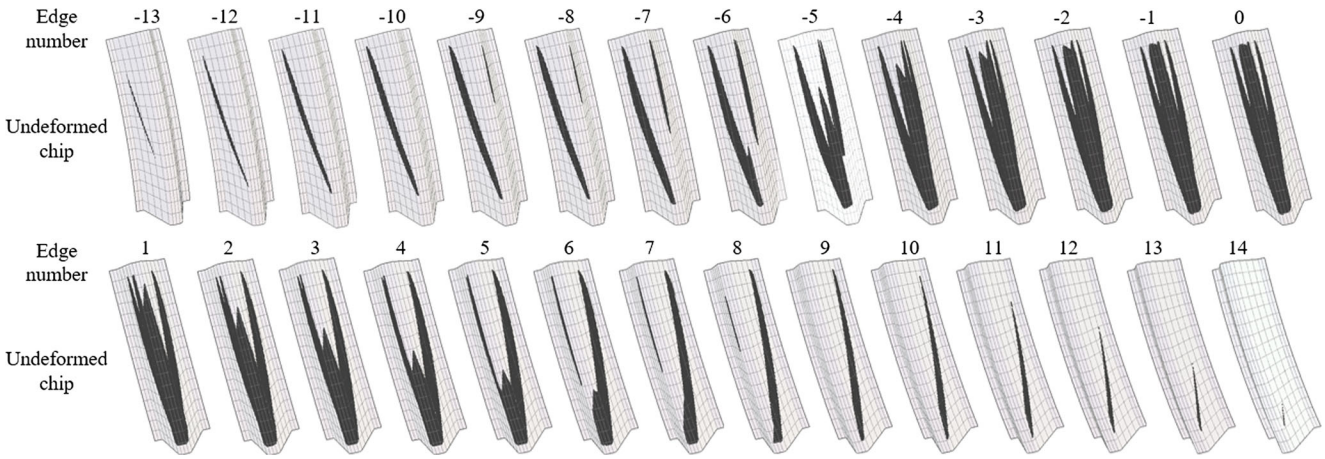

Fig. 6 The shape of undeformed chips removed by each effective cutting edge during gear hobbing [26]

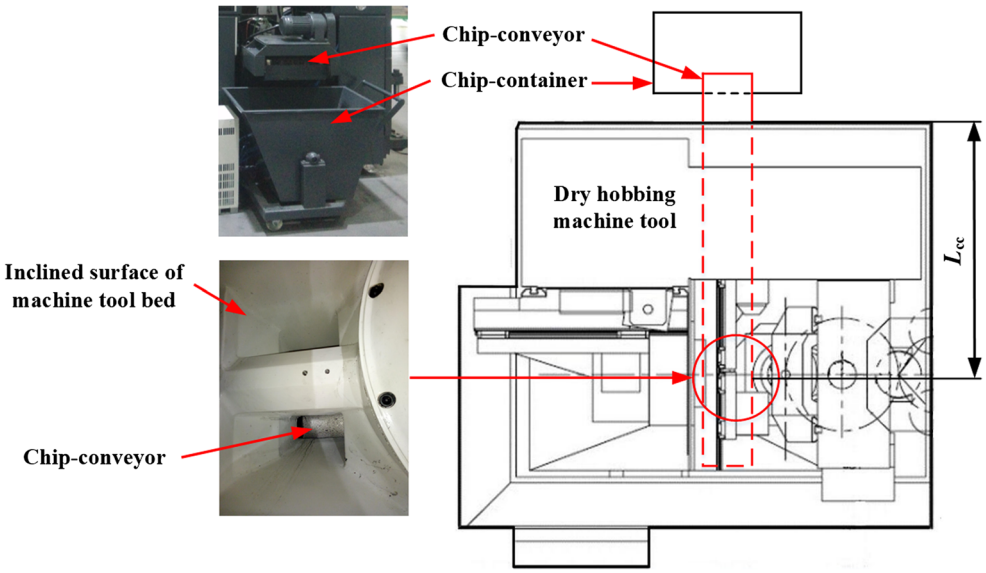

Fig. 7 Sketch of chip conveyor and chip container of dry hobbing machine tool (top view)

two nozzles generally: one is hanged above the hob and the other one is hanged above the workpiece.

Compressed cold air is sent to the cutting zone during hobbing. After one workpiece is processed, in a certain time, a specific part of compressed cold air, which is far from the cutting zone, will be in steady state. That means its macroscopic velocity approaches nearly zero, and its temperature approaches T_{ia}. Considering the first law of thermodynamics, when compressed cold air comes out of the nozzles, its energy is calculated as

$$E_A = U_A + E_{k,A} + E_{p,A} \tag{15}$$

where U_A is the internal energy of compressed cold air, $E_{k,A}$ is the kinetic energy of compressed cold air, and $E_{p,A}$ is the gravitational potential energy of compressed cold air.

The energy change of machine tool, ΔU_A, that is caused by compressed cold air, could be gained by calculating the difference of thermal energy between compressed cold air and the same mass of interior space air in steady state, that is,

$$\Delta U_A = \sum_{h=1}^{n_2} \int_0^t c_A \dot{m}_{A,h} \left(T_{ia} - T_{A,h}\right) dt \tag{16}$$

where c_A is the specific heat capacity of compressed cold air, h is the no. of corresponding nozzles, $m_{A,h}$ is the mass flow rate of compressed cold air in corresponding nozzle, and $T_{A,h}$ is the temperature of compressed cold air when it comes out of the corresponding nozzle.

The mass flow rate of ambient air that flows into dry hobbing machine tool, m_D, is produced by

$$\dot{m}_D = \dot{m}_E - \sum_{h=1}^{n_2} \dot{m}_{A,h} \tag{17}$$

where m_E is the mass flow rate of air which flows into the air extraction and filtration device.

The thermal energy change of dry hobbing machine tool that is caused by airflow between interior space and ambient is calculated as

$$\Delta U_D = \int_0^t c_A \left(\dot{m}_E - \sum_{h=1}^{n_2} \dot{m}_{A,h} \right) (T_{ia} - T_a) dt \tag{18}$$

where T_a is the ambient temperature.

When the macroscopic velocity of compressed cold air approaches nearly zero, the kinetic energy change of it can be determined as

$$\Delta E_{k,A} = -\sum_{h=1}^{n_2} \int_0^t 0.5 \dot{m}_{A,h} v_{A,h}^2 dt \tag{19}$$

where v_{Ah} is the velocity of compressed cold air when it comes out of the corresponding nozzle.

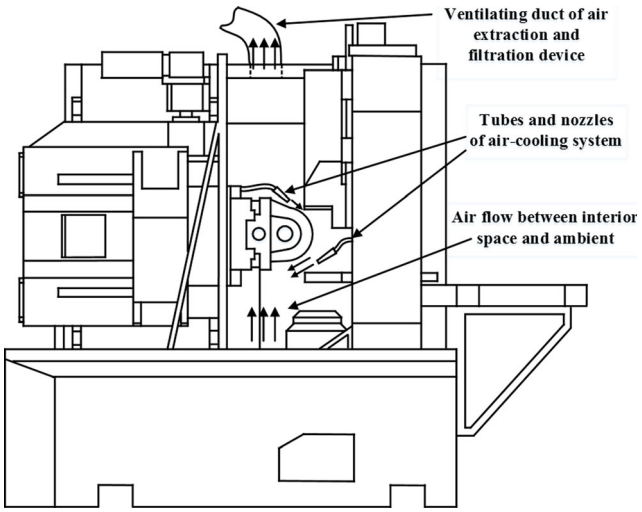

Fig. 8 Schematic of airflow in dry hobbing machine tool (front view)

The change of gravitational potential energy could be neglected, that is,

$$\Delta E_{\mathrm{p,A}} = 0 \tag{20}$$

The thermal energy change of dry hobbing machine tool that is caused by airflow, ΔE_{A}, can be calculated as

$$\begin{aligned}\Delta E_{\mathrm{A}} &= \Delta U_{\mathrm{D}} + \Delta U_{\mathrm{A}} + \Delta E_{\mathrm{k,A}} + \Delta E_{\mathrm{p,A}} \\ &= \int_0^t \left[c_{\mathrm{A}} \left(\dot{m}_{\mathrm{E}} - \sum_{h=1}^{n_2} \dot{m}_{\mathrm{A},h} \right) (T_{\mathrm{ia}} - T_{\mathrm{a}}) + \sum_{h=1}^{n_2} c_{\mathrm{A}} \dot{m}_{\mathrm{A},h} (T_{\mathrm{ia}} - T_{\mathrm{A},h}) - \sum_{h=1}^{n_2} 0.5 \dot{m}_{\mathrm{A},h} v_{\mathrm{A},h}^2 \right] dt\end{aligned} \tag{21}$$

3.5 Thermal energy change caused by motor coolant

The major thermal energy sink in motor component is mainly caused by motor coolant flow and bearing lubricant flow. Commonly, motor cooling system is based on a closed-loop cooling system where the coolant is cooling down in an external refrigeration and then pumped back into the motor. The motor coolant fluids are forced to circulate through various zones of the headstock and spindle structure to cool the spindle. Figure 9 shows the frame of FANUC synchronous built-in spindle motor which is used as the tool spindle. The cooling groove is placed at some kind of phase on the periphery of the stator jacket. The motor coolant moves at a flow rate in the cooling groove. Convection heat transfer occurs at the surface of the cooling groove on the stator jacket.

The motor coolant enters dry hobbing machine tool in n_3 circulations. Thermal energy that convects into motor coolant, ΔE_{Mc}, is found as

$$\Delta E_{\mathrm{Mc}} = \sum_{g=1}^{n_3} \int_0^t c_{\mathrm{M}} \dot{m}_{\mathrm{M},g} \left(T_{\mathrm{M},g,\mathrm{o}} - T_{\mathrm{M},g,\mathrm{e}} \right) dt \tag{22}$$

where g is the no. of corresponding motor coolant circulation in dry hobbing machine tool, c_{M} is the specific heat capacity of motor coolant, $m_{\mathrm{M},g}$ is the flow rate of motor coolant in corresponding circulation, $T_{\mathrm{M},g,\mathrm{o}}$ is the temperature of motor coolant when it comes out of corresponding circulation, and $T_{\mathrm{M},g,\mathrm{e}}$ is the temperature of motor coolant when it enters corresponding circulation.

3.6 Thermal energy change caused by lubricating oil

The lubricating station, which is placed at the outside of the dry hobbing machine tool, is mainly composed of cooling device, lubricating oil container, filter, motor, control parts, pressure and flow detection parts, etc. The lubricating oil that comes out of the lubricating station separates into n_4 circulations to enter the dry hobbing machine tool components, such as spindle component and workpiece table component. The thermal energy that transfers into the lubricating oil by convection, ΔE_{L}, is found as

$$\Delta E_{\mathrm{L}} = \sum_{k=1}^{n_4} \int_0^t c_{\mathrm{L}} \dot{m}_{\mathrm{L},k} \left(T_{\mathrm{L},k,\mathrm{o}} - T_{\mathrm{L},k,\mathrm{e}} \right) dt \tag{23}$$

where k is the no. of lubricating oil circulation, c_{L} is the specific heat capacity of lubricating oil, $m_{\mathrm{L},k}$ is the flow rate of lubricating oil in corresponding circulation, $T_{\mathrm{L},k,\mathrm{o}}$ is the temperature of lubricating oil when it comes out of corresponding circulation, and $T_{\mathrm{L},k,\mathrm{e}}$ is the temperature of lubricating oil when it enters corresponding circulation.

3.7 Thermal energy sink caused by hydraulic oil

The hydraulic station, which is placed outside of dry hobbing machine tool, is mainly composed of cooling device,

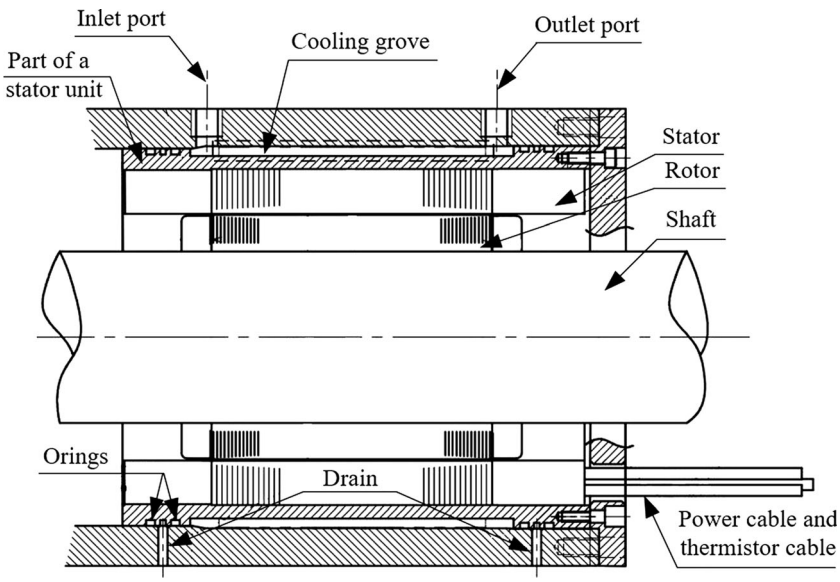

Fig. 9 Example of a motorized spindle sketch

hydraulic oil container, filter, hydraulic pump, electromagnetic valve, solenoid valve, motor, etc. The hydraulic oil that comes out from the dry hobbing machine tool is cooling down in the hydraulic station and then enters the dry hobbing machine tool to form a loop system. The main hydraulic parts in dry hobbing machine tool are the following:

1. Hob arbor cylinder, tailstock cylinder, hob head swivel cylinder, etc.
2. Workpiece clamp cylinder

The thermal energy that is generated by hydraulic parts in dry hobbing machine tool is relatively small, so that it could be neglected to simplify the model. The thermal energy sink that is caused by hydraulic oil is mainly thermal energy that transfers into the lubricating oil by convection. Hydraulic oil comes out of the hydraulic station through one tube and is then divided into n_5 circulations to enter the dry hobbing machine tool. Thermal energy that transfers into the hydraulic oil by convection, ΔE_{H}, is found as

$$\Delta E_{\mathrm{H}} = \sum_{l=1}^{n_5} \int_0^t c_{\mathrm{H}} \dot{m}_{\mathrm{H},l} \left(T_{\mathrm{H},l,\mathrm{o}} - T_{\mathrm{H},l,\mathrm{e}}\right) dt \tag{24}$$

where l is the no. of corresponding circulation, c_{H} is the specific heat capacity of hydraulic oil, $m_{\mathrm{H},l}$ is the flow rate of hydraulic oil in corresponding circulation, $T_{\mathrm{H},l,\mathrm{o}}$ is the temperature of hydraulic oil when it comes out of outlet port of corresponding circulation, and $T_{\mathrm{H},l,\mathrm{e}}$ is the temperature of cooling medium when it enters corresponding circulation.

3.8 Heat convection through dry hobbing machine tool surface

The thermal energy that is lost by convection between dry hobbing machine tool surface and ambient air should be taken into consideration. For most dry hobbing machine tool, the shape of them could be simplified to a cuboid. And the surface thermal energy is lost by free convection from vertical sides, horizontal top, and horizontal bottom. As the ambient air could be seemed as quiescent, the thermophysical properties of air at atmospheric pressure are as follows [28]: $k = 26.3 \times 10^{-3}$ W/m K, $\nu = 15.89 \times 10^{-6}$ m^2/s, $\alpha = 22.5 \times 10^{-6}$ m^2/s, Pr = 0.707, and $\beta = 1/T_f = 2/(T_{\mathrm{s}} + T_{\mathrm{a}})$. The Rayleigh number is determined as

$$\begin{aligned} \mathrm{Ra}_L &= \frac{g\beta(T_{\mathrm{s}} - T_{\mathrm{a}})L^3}{\alpha\nu} \\ &= \frac{9.8 \times 2 \times (T_{\mathrm{s}} - T_{\mathrm{a}}) \times L^3}{22.5 \times 10^{-6} \times 15.89 \times 10^{-6} \times (T_{\mathrm{s}} + T_{\mathrm{a}})} \\ &= 5.482 \times 10^{10} \frac{T_{\mathrm{s}} - T_{\mathrm{a}}}{T_{\mathrm{s}} + T_{\mathrm{a}}} L^3 \end{aligned} \tag{25}$$

where T_{s} is the temperature of dry hobbing machine tool surface; the temperature of dry hobbing machine tool surface or ambient air could be regarded as uniform.

For the four sides of dry hobbing machine tool, L in Eq. (25) refers to H which is shown in Fig. 10.

Generally, T_{a} ranges from about 263 to about 313 K and the difference between T_{s} and T_{a} ranges from about 0 to about 20 K, according to actual production experience. Thus, Eq. (26) could be obtained.

$$\frac{\mathrm{Ra}_L}{\mathrm{Ra}_{x,c}} > 1 \tag{26}$$

where $\mathrm{Ra}_{x,c}$ is the critical Rayleigh number of vertical plates and $\mathrm{Ra}_{x,c} \approx 10^9$.

From Eq. (26), it follows that transition to turbulence occurs on the four sides. Thus, for the four sides, the average Nusselt number is then given by [29].

$$\begin{aligned} \overline{\mathrm{Nu}}_{L,\mathrm{S}} &= \left\{ 0.825 + \frac{0.387 \mathrm{Ra}_L{}^{1/6}}{\left[1 + (0.492/\mathrm{Pr})^{9/16}\right]^{8/27}} \right\}^2 \\ &= \left\{ 0.825 + 19.956 H^{1/2} \left(\frac{T_{\mathrm{s}} - T_{\mathrm{a}}}{T_{\mathrm{s}} + T_{\mathrm{a}}} \right)^{1/6} \right\}^2 \end{aligned} \tag{27}$$

For the top plate and the bottom plate, the characteristic length is calculated as [30].

$$L = \frac{\mathrm{A}_{\mathrm{s},1}}{P} = \frac{L_{\mathrm{a}} \cdot L_{\mathrm{b}}}{2(L_{\mathrm{a}} + L_{\mathrm{b}})} \tag{28}$$

where $A_{\mathrm{s},1}$ is the surface area of the top plate or bottom plate and P is the perimeter of the top plate or bottom plate.

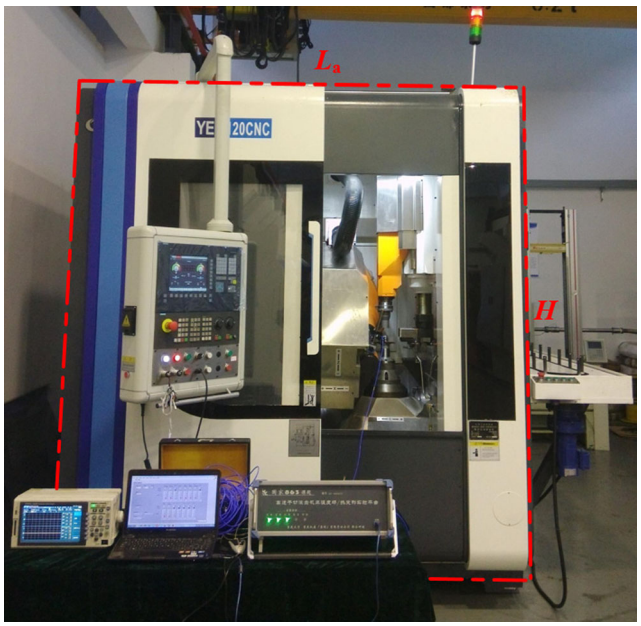

Fig. 10 Schematic diagram of dry hobbing machine tool dimension

And the average Nusselt number for the top plate is then given by

$$\overline{\mathrm{Nu}}_{L,1} = 0.15\mathrm{Ra}_L{}^{1/3} = 569.820\mathrm{H}\left(\frac{T_\mathrm{s}-T_\mathrm{a}}{T_\mathrm{s}+T_\mathrm{a}}\right)^{1/3} \tag{29}$$

As the bottom of machine tool has a certain distance with the ground, heat transfer by convection between the bottom and ambient air could be calculated by the similar method. The average Nusselt number is given by

$$\overline{\mathrm{Nu}}_{L,2} = 0.27\mathrm{Ra}_L{}^{1/4} = 130.647\mathrm{H}^{3/4}\left(\frac{T_\mathrm{s}-T_\mathrm{a}}{T_\mathrm{s}+T_\mathrm{a}}\right)^{3/4} \tag{30}$$

The convection coefficient is calculated as

$$\overline{h} = \frac{\overline{\mathrm{Nu}}_L \cdot k}{L} = 26.3\times10^{-3}\frac{\overline{\mathrm{Nu}}_L}{L} \tag{31}$$

The rate of heat transfer by free convection from one plate to ambient can be obtained from Newton's law of cooling.

$$q = \overline{h}A_\mathrm{s}(T_\mathrm{s}-T_\mathrm{a}) = 26.3\times10^{-3}\frac{\overline{\mathrm{Nu}}_L A_\mathrm{s}(T_\mathrm{s}-T_\mathrm{a})}{L} \tag{32}$$

The rate of thermal energy loss of dry hobbing machine tool surface is calculated as

$$\begin{aligned} q_\mathrm{M} &= 2(q_{\mathrm{s}1}+q_{\mathrm{s}2})+q_1+q_2 \\ &= 52.6\times10^{-3}(L_\mathrm{a}+L_\mathrm{b})(T_\mathrm{s}-T_\mathrm{a})\left(\overline{\mathrm{Nu}}_{L,\mathrm{S}}+\overline{\mathrm{Nu}}_{L,1}+\overline{\mathrm{Nu}}_{L,2}\right) \end{aligned} \tag{33}$$

Thus, the thermal energy that is lost by convection between dry hobbing machine tool surface and ambient, ΔE_C, can be calculated as

$$\Delta E_\mathrm{C} = \int_0^t q_\mathrm{M}dt = F(T_\mathrm{s}, T_\mathrm{a}, H, L_\mathrm{a}, L_\mathrm{b}, t) \tag{34}$$

3.9 Radiation

As shown in Fig. 11, from a radiation balance on the medium, it follows that [19]

$$G_\lambda = G_{\lambda,\mathrm{ref}} + G_{\lambda,\mathrm{abs}} + G_{\lambda,\mathrm{tr}} \tag{35}$$

where spectral irradiation G_λ (W/m^2 μm) is the rate at which radiation of wavelength, λ, is incident on a surface per unit area of the surface and per unit wavelength interval $d\lambda$ about λ, $G_{\lambda,\mathrm{ref}}$ is the absorbed portion of G_λ, $G_{\lambda,\mathrm{abs}}$ is the absorbed portion of G_λ, and $G_{\lambda,\mathrm{tr}}$ is the transmitted portion of G_λ.

For opaque medium, there is no transmitted portion of G_λ, that is, $G_{\lambda,\mathrm{tr}} = 0$. In dry hobbing machine tool, there is a massive metal shield, which is opaque. And the semitransparent medium, window of machine tool gates, is relatively small; thus, the part of radiation energy that is lost by transmission can be neglected.

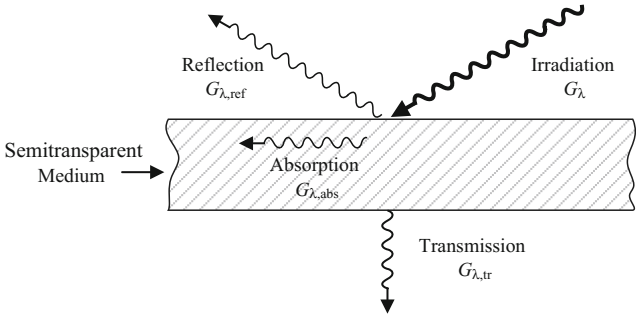

Fig. 11 Absorption, reflection, and transmission processes associated with a semitransparent medium [19]

Thus, thermal energy that is lost by radiation is mainly caused by the radiation between dry hobbing machine tool shell and workshop walls. The surface emissive power can be found as

$$q_\mathrm{R} = \frac{\sigma A_1\left(T_\mathrm{s}{}^4 - T_2{}^4\right)}{\frac{1}{\varepsilon_1}+\frac{A_1}{A_2}\left(\frac{1}{\varepsilon_2}-1\right)} \tag{36}$$

where A_1 is the surface area of dry hobbing machine tool shell, ε_1 is the emissivity of dry hobbing machine tool shell, A_2 is the surface area of workshop walls, T_2 is the temperature of workshop walls, ε_2 is the emissivity of workshop walls, σ is the *Stefan–Boltzmann* constant, and $\sigma = 5.670\times10^{-8}$ W/m^2 K^4.

Under the condition that $A_2 \gg A_1$, and T_2 is close to T_a, thermal energy that is lost by radiation can be found as

$$E_\mathrm{R} = \int_0^t q_\mathrm{R}dt = \int_0^t \sigma A_1\varepsilon_1\left(T_\mathrm{s}{}^4 - T_\mathrm{a}{}^4\right)dt \tag{37}$$

3.10 Multi-variable thermal energy control model

In this paper, t is the running time of dry hobbing machine tool from starting to a point that is picked at which hob and workpiece are still. Thus, Eqs. (38) and (39) could be obtained.

$$\Delta E_\mathrm{p} = -\Delta E_{\mathrm{p,ch}} \tag{38}$$

$$\Delta E_\mathrm{k} = 0 \tag{39}$$

According to Eqs. (4), (5), (6), (7), (21), (22), (23), (24), (34), (37), (38), and (39), the thermal energy change of dry hobbing machine tool, that is, the multi-variable driving thermal energy control model, is produced by

$$\begin{aligned} \Delta U = {} & E_\mathrm{T} + \Delta E_{\mathrm{p,ch}} - \Delta E_\mathrm{C} - \Delta E_{\mathrm{Wp}} - E_\mathrm{R} \\ & -(\Delta E_\mathrm{L} + \Delta E_{\mathrm{Mc}} + \Delta E_\mathrm{H} + \Delta E_\mathrm{A} + \Delta E_{\mathrm{Ch}}) \end{aligned} \tag{40}$$

The thermal energy control model shows the heat generation and sink of the dry hobbing machine tool. It is a kind of real-time model which is suitable for the calculation of thermal

accumulation energy of dry hobbing machine tool. In recent years, monitoring sensors, such as thermal sensors, flowmeters, and power monitor, are mounted on dry hobbing machine tool for condition monitoring. Thus, temperature variables, mass flow rate variables, power variables, etc. are used in the thermal energy control model, in order to make the required variables' value that could be measured in a convenient way. The simplification of this model is for purpose of easier application.

4 Application method and optimization of control variables

4.1 Application method

An application method is proposed to optimize control variables according to the time history of the thermal energy that accumulated in dry hobbing machine tool in real time, with the thermal energy control model. The method incorporates a multi-objective optimization algorithm, which is used for optimization of control variables.

The thermal energy control model shows the control variables of dry hobbing machine tool. When the type of workpiece and process parameters remain unchanged, the following parameters could be seemed as constant: c_A, c_M, c_L, c_H, c_{wp}, c_{ch}, H, L_a, L_b, L_{cc}, z, m_{wp}, m_{ch}, n_2, n_3, n_4, and n_5. And the following kinds of parameters are variable:

1. P_i
2. $m_{M,g}, m_{L,k}, m_{H,l}, m_{A,h}, m_E$
3. $T_{M,g,e}, T_{M,g,o}, T_{L,k,e}, T_{L,k,o}, T_{H,l,e}, T_{H,l,o}, T_{A,h}, T_{ia}, T_s, T_a, T_{wp2,j}, T_{wp1,j}, T_{ch2,j}, T_{ch}$
4. t, n_1, u_{cc}

The control variables are as follows: $T_{M,g,e}$, $T_{L,k,e}$, $T_{H,l,e}$, $T_{A,h}$, $m_{M,g}$, $m_{L,k}$, $m_{H,l}$, $m_{A,h}$, m_E, and u_{cc}. Equation (40) can be expressed as

$$\Delta U = \Delta E_{mea} - \Delta E_{con} \tag{41}$$

$$\Delta E_{con} = \Delta E_L + \Delta E_W + \Delta E_H + \Delta E_A + \Delta E_{Ch} \tag{42}$$

$$\Delta E_{mea} = E_T + \Delta E_{p,ch} - \Delta E_C - \Delta E_{wp} - E_R \tag{43}$$

where ΔE_{con} is the part of ΔU that could be adjusted by changing the value of control variables.

In this paper, the optimization cycle, t_o is integral multiple of production cycle, t_p. Thus, when optimization is applied, t can be expressed as

$$t = bt_o + t_\delta = bat_p + t_\delta \tag{44}$$

where a is an integer, b is an integer variable, and t_δ is the time interval from the time point that the spindles are warmed up to the time point that the process is started.

Equation (41) can be expressed as

$$\Delta U_b = \Delta E_{mea,b} - \Delta E_{con,b} \tag{45}$$

where ΔU_b is the thermal energy accumulation value of dry hobbing machine tool when $t = bt_o + t_\delta$, $\Delta E_{mea,b}$ is the value of ΔE_{mea} when $t = bt_o + t_\delta$, and $\Delta E_{con,b}$ is the value of ΔE_{con} when $t = bt_o + t_\delta$.

The flowchart of the application method is shown Fig. 12.

During processing, the following variables are measured by thermal sensors: $T_{M,g,e}$, $T_{M,g,o}$, $T_{L,k,e}$, $T_{L,k,o}$, $T_{H,l,e}$, $T_{H,l,o}$, $T_{A,h}$, T_{ia}, T_s, T_a, $T_{wp2,j}$, $T_{wp1,j}$, $T_{ch2,j}$, T_{ch}. $m_{M,g}$, $m_{L,k}$, $m_{H,l}$, $m_{A,h}$, and m_E are measured by flowmeters, and P_i is measured by a power analyzer. When $t = bt_o + t_\delta$, ΔU_b is calculated using the thermal energy control model and measuring data. The aim of optimization is to make ΔU_{b+1} approaches 0, that is,

$$\begin{aligned} \Delta E_{mea,b+1} - \Delta E_{con,b+1} &= \Delta E_{mea,b} + \left(\Delta E_{mea,b+1} - \Delta E_{mea,b}\right) - \Delta E_{con,b} \\ &\quad - \left(\Delta E_{con,b+1} - \Delta E_{con,b}\right) = \Delta U_b + \left(\Delta E_{mea,b+1} - \Delta E_{mea,b}\right) \\ &\quad - \left(\Delta E_{con,b+1} - \Delta E_{con,b}\right) = 0 \end{aligned} \tag{46}$$

where ΔU_{b+1} is the thermal energy accumulation value of dry hobbing machine tool when $t = (b+1)\, t_o + t_\delta$, $\Delta E_{mea,b+1}$ is the value of ΔE_{mea} when $t = (b+1)\, t_o + t_\delta$, and $\Delta E_{con,b+1}$ is the value of ΔE_{con} when $t = (b+1)\, t_o + t_\delta$.

As $\Delta E_{mea,b+1} - \Delta E_{mea,b}$ is obtained by measuring after optimization, $\Delta E_{mea,b} - \Delta E_{mea,b-1}$ is used as the

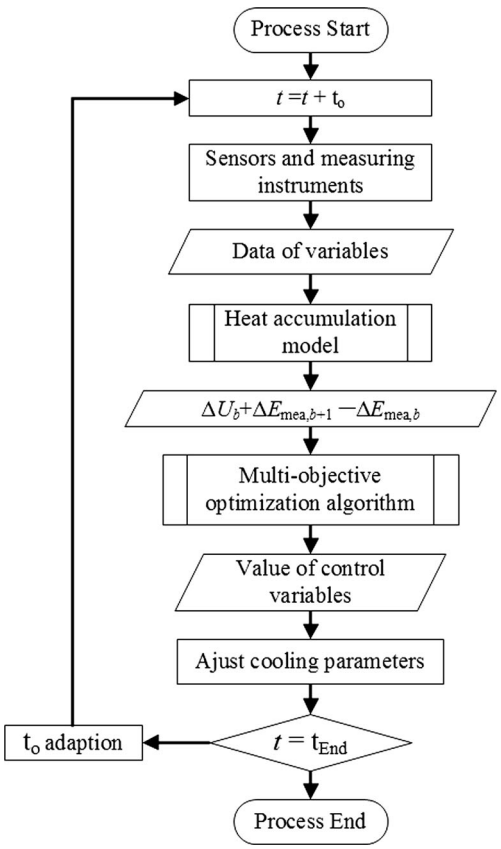

Fig. 12 Flowchart of the application method

approximate value of $\Delta E_{\mathrm{mea},b+1} - \Delta E_{\mathrm{mea},b}$. Thus, Eq. (47) can be obtained.

$$\Delta E_{\mathrm{con},b+1} - \Delta E_{\mathrm{con},b} = \Delta E_{\mathrm{mea},b} - \Delta E_{\mathrm{mea},b-1} + \Delta U_b \tag{47}$$

The value of $T_{\mathrm{M},g,\mathrm{o}}$, $T_{\mathrm{L},k,\mathrm{o}}$, $T_{\mathrm{H},l,\mathrm{o}}$, and T_{ia}, when $t = bt_{\mathrm{o}} + t_{\delta}$, is used as the approximate value of those variables during the next optimization cycle.

The thermal energy lost which is caused by removing of chips from one workpiece, $\Delta E_{\mathrm{Ch},1}$, is produced by

$$\Delta E_{\mathrm{Ch},1} = c_{\mathrm{ch}} m_{\mathrm{ch}} \left(T_{\mathrm{ch}2,1} - T_{\mathrm{wp}1,1} \right) \tag{48}$$

For another workpiece, the thermal energy lost which is caused by removing of chips, $\Delta E_{\mathrm{Ch},2}$, could be calculated as

$$\Delta E_{\mathrm{Ch},2} = Q_{\mathrm{Ch},2} - Q_{\mathrm{Ch},1} + \Delta E_{\mathrm{Ch},1} \tag{49}$$

Thus, in Eq. (47), there is

$$\Delta E_{\mathrm{Ch},b+1} - \Delta E_{\mathrm{Ch},b} = a\left(Q_{\mathrm{Ch},b} - Q_{\mathrm{Ch},b-1} \right) + \Delta E_{\mathrm{Ch},b} - \Delta E_{\mathrm{Ch},b-1} \tag{50}$$

4.2 Optimization of control variables

A multi-objective optimization algorithm is proposed to determine the value of control variables, combined with the thermal energy control model. Due to its growing economic relevance and the related environmental impact, power consumption is a major issue in both politics and companies nowadays [31]. Optimization is realized by changing the value of control variables, which will lead to power cost change and cooling medium consumption cost change. Thus, the corresponding power cost and cooling medium consumption cost are considered as objectives. The power cost of corresponding device, C_{P}, is calculated as

$$C_{\mathrm{P}} = \int_0^{t_{\mathrm{o}}} C_{\mathrm{e}} (P_{\mathrm{L}} + P_{\mathrm{M}} + P_{\mathrm{H}} + P_{\mathrm{Ad}} + P_{\mathrm{Ae}} + P_{\mathrm{Ch}}) dt \tag{51}$$

where C_{e} is the electricity price per kilowatt-hour, P_{L} is the power of lubricating oil cooling device which is the function of $T_{\mathrm{L},k,\mathrm{e}}$, $T_{\mathrm{L},k,\mathrm{o}}$,and $m_{\mathrm{L}k}$, P_{M} is the power of motor coolant cooling device which is the function of $T_{\mathrm{M},g,\mathrm{e}}$, $T_{\mathrm{M},g,\mathrm{o}}$, and $m_{\mathrm{M},g}$, P_{H} is the power of hydraulic oil cooling device which is the function of $T_{\mathrm{H},\,l,\mathrm{e}}$, $T_{\mathrm{H},l,\mathrm{o}}$, and $m_{\mathrm{H},l}$, P_{Ad} is the power of refrigerated air dryer which is the function of $T_{\mathrm{A},h}$ and $m_{\mathrm{A},h}$, P_{Ae} is the power of air extraction and filtration device which is the function of m_{E}, and P_{Ch} is the power of chip conveyor which is the function of u_{cc}.

As the makeup rate of motor coolant, lubricating oil, and hydraulic oil is relatively little, the change of cooling medium consumption cost is mainly caused by consumption of compressed air, C_{c}, which could be calculated as

$$C_{\mathrm{c}} = \int_0^{t_{\mathrm{o}}} \mathrm{C}_{\mathrm{pc}} \cdot V_{\mathrm{A}} dt \tag{52}$$

where C_{pc} is the price of compressed air per cubic meter and V is the volume consumption rate of compressed air which is the function of $m_{\mathrm{A},h}$.

The corresponding power cost and cooling medium consumption cost, C, could be calculated by

$$C = C_{\mathrm{P}} + C_{\mathrm{c}} \tag{53}$$

The aim of cooling parameter optimization is minimizing thermal energy accumulation of dry hobbing machine tool and the corresponding power and cooling medium consumption cost. Thus, the objective is denoted by

$$\Delta E_{\mathrm{con},b+1} - \Delta E_{\mathrm{con},b} = \Delta E_{\mathrm{mea},b} - \Delta E_{\mathrm{mea},b-1} + \Delta U_b \tag{54}$$

$$\min \quad C = C_{\mathrm{P}} + C_{\mathrm{c}} \tag{55}$$

Decision variables, i.e., control variables, are as follows: $T_{\mathrm{M},g,\mathrm{e}}$, $T_{\mathrm{L},k,\mathrm{e}}$, $T_{\mathrm{H},l,\mathrm{e}}$, $T_{\mathrm{A},h}$, $m_{\mathrm{M},g}$, $m_{\mathrm{L},k}$, $m_{\mathrm{H},l}$, $m_{\mathrm{A}h}$, m_{E}, and u_{cc}. The constraints of decision variables can be obtained as follows:

$$T_{\mathrm{M},g,\mathrm{e},\min} \le T_{\mathrm{M},g,\mathrm{e}} \le T_{\mathrm{M},g,\mathrm{e},\max} \tag{56}$$

$$T_{\mathrm{L},k,\mathrm{e},\min} \le T_{\mathrm{L},k,\mathrm{e}} \le T_{\mathrm{L},k,\mathrm{e},\max} \tag{57}$$

$$T_{\mathrm{H},l,\mathrm{e},\min} \le T_{\mathrm{H},l,\mathrm{e}} \le T_{\mathrm{H},l,\mathrm{e},\max} \tag{58}$$

$$T_{\mathrm{A},h,\min} \le T_{\mathrm{A},h} \le T_{\mathrm{A},h,\max} \tag{59}$$

$$\dot{m}_{\mathrm{M},g,\min} \le \dot{m}_{\mathrm{M},g} \le \dot{m}_{\mathrm{M},g,\max} \tag{60}$$

$$\dot{m}_{\mathrm{L},k,\min} \le \dot{m}_{\mathrm{L},k} \le \dot{m}_{\mathrm{L},k,\max} \tag{61}$$

$$\dot{m}_{\mathrm{H},l,\min} \le \dot{m}_{\mathrm{H},l} \le \dot{m}_{\mathrm{H},l,\max} \tag{62}$$

$$\dot{m}_{\mathrm{A},h,\min} \le \dot{m}_{\mathrm{A},h} \le \dot{m}_{\mathrm{A},h,\max} \tag{63}$$

$$\dot{m}_{\mathrm{E},\min} \le \dot{m}_{\mathrm{E}} \le \dot{m}_{\mathrm{E},\max} \tag{64}$$

$$u_{\mathrm{cc},\min} \le u_{\mathrm{cc}} \le u_{\mathrm{cc},\max} \tag{65}$$

In the application of control variable optimization problem of dry hobbing machine tool, limitations of control variables are emanating from the technical view points. For example, the allowable liquid velocity in the tube should be within a range to prevent fouling and erosion, respectively. In industrial production, the constraints of control variables are affected by dry hobbing machine tool status, cooling device parameters, tube parameters, temperature limitation, ambient temperature, etc.

5 Verification

Experiments were carried out on a dry hobbing machine tool to verify the effect of the application of thermal energy control model. The workpiece is a kind of gear that is used in car

transmission. Measuring instruments are shown as follows: Pt-100 thermal resistances, infrared camera, flowmeters, power analyzer, data acquisition device, computer, timer, etc. Before the experiments, those sensors and device were calibrated. The material emissivity of workpiece and chip, which would be used to set the parameter of the infrared camera, was calibrated too. The data acquisition device was composed of National Instruments data acquisition system. The data acquisition software was programmed in LabVIEW.

In the experiment that the model was applied, the dry hobbing machine tool kept running about 3 h. The timer was started when the spindles have been warmed up. The optimization cycle is 360 s, which is five times of production cycle. The following kinds of data were recorded during experiments: P_i, $T_{\mathrm{M},g,\mathrm{e}}$, $T_{\mathrm{M},g,\mathrm{o}}$, $T_{\mathrm{L},k,\mathrm{e}}$, $T_{\mathrm{L},k,\mathrm{o}}$, $T_{\mathrm{H},l,\mathrm{e}}$, $T_{\mathrm{H},l,\mathrm{o}}$, $T_{\mathrm{A},h}$, T_{ia}, T_{s}, T_{a}, $T_{\mathrm{wp2},j}$, $T_{\mathrm{wp1},j}$, $T_{\mathrm{ch2},j}$, T_{ch}, $m_{\mathrm{M},g}$, $m_{\mathrm{L},k}$, $m_{\mathrm{H},l}$, $m_{\mathrm{A}h}$, m_{E}, t, n_1, and u_{cc}. Those data were recorded and used to calculate ΔU with the thermal energy control model every 360 s. Values of control variables, that is, $T_{\mathrm{M},g,\mathrm{e}}$, $T_{\mathrm{L},k,\mathrm{e}}$, $T_{\mathrm{H},l,\mathrm{e}}$, $T_{\mathrm{A},h}$, $m_{\mathrm{M},g}$, $m_{\mathrm{L},k}$, $m_{\mathrm{H},l}$, $m_{\mathrm{A}h}$, m_{E}, and u_{cc}, were determined using the multi-objective optimization algorithm.

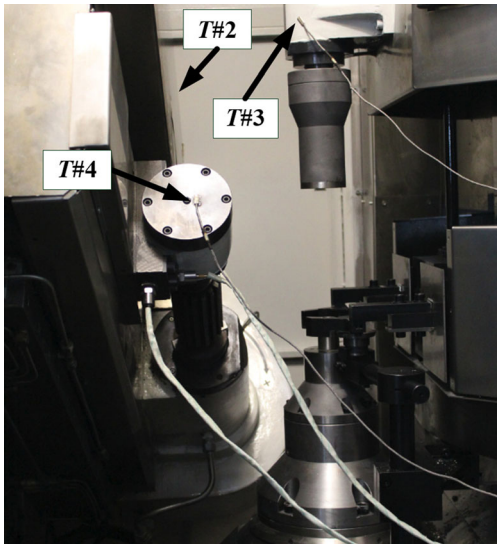

Fig. 13 Locations of thermal resistances that are used for validation

For example, when t = 1440 s, $\Delta E_{\mathrm{mea},1440} - \Delta E_{\mathrm{mea},1080} + \Delta U_{1440}$ could be calculated according to Eqs. (40) and (43). Thus, Eq. (47) could be expressed as

$$\begin{aligned}&\sum_{k=1}^{n_4}\int_{1440}^{1800} c_{\mathrm{L}} m_{\mathrm{L},k}\left(T_{\mathrm{L},k,\mathrm{o}} - T_{\mathrm{L},k,\mathrm{e}}\right)dt + \sum_{g=1}^{n_3}\int_{1440}^{1800} c_{\mathrm{M}} m_{\mathrm{M},g}\left(T_{\mathrm{M},g,\mathrm{o}} - T_{\mathrm{M},g,\mathrm{e}}\right)dt + \sum_{l=1}^{n_5}\int_{1440}^{1800} c_{\mathrm{H}} m_{\mathrm{H},l}\left(T_{\mathrm{H},l,\mathrm{o}} - T_{\mathrm{H},l,\mathrm{e}}\right)\\ &+\int_{1440}^{1800}\left[c_{\mathrm{A}}\left(\dot{m}_{\mathrm{E}} - \sum_{h=1}^{n_2} m_{\mathrm{A},h}\right)\left(T_{\mathrm{ia}} - T_{\mathrm{a}}\right)\right]dt + \sum_{h=1}^{n_2}\int_{1440}^{1800} c_{\mathrm{A}} m_{\mathrm{A},h}\left(T_{\mathrm{ia}} - T_{\mathrm{A},h}\right)dt - \sum_{h=1}^{n_2}\int_{1440}^{1800} 0.5 m_{\mathrm{A},h} v_{\mathrm{A},h}^2 dt \qquad (66)\\ &+5\left(Q_{\mathrm{Ch},1440} - Q_{\mathrm{Ch},1080}\right) + \Delta E_{\mathrm{Ch},1440} - \Delta E_{\mathrm{Ch},1080} = \Delta E_{mea,1440} - \Delta E_{mea,1080} + \Delta U_{1440}\end{aligned}$$

As value of $T_{\mathrm{L},k,\mathrm{o}}$, $T_{\mathrm{M},g,\mathrm{o}}$, $T_{\mathrm{H},l,\mathrm{o}}$, and $\mathrm{T_{L,k,o}}$ during the next optimization cycle are obtained by measuring after optimization, the values of them, when t = 1440 s, are used as the approximate value of those variables during the next optimization cycle. Then, value of decision variables could be obtained using Eq. (66) and the multi-objective optimization algorithm.

For comparing, in another experiment, the same dry hobbing machine tool kept running for about 3 h without control variable optimization.

Four thermal resistances were mounted on the dry hobbing machine tool to validate the effect of the thermal energy control model and the application method. The locations and corresponding temperature variables of those thermal resistances are shown in Fig. 13, where *T*#1 is the temperature of ambient, *T*#2 is the temperature of thermal resistance that was suspended in the machine tool (close to machine tool shield), *T*#3 is the temperature of thermal resistance that was mounted on the surface of workpiece column, and *T*#4 is the temperature of thermal resistance that was mounted on the surface of anterior end cover of the hob spindle. Infrared thermal camera was used to obtain the thermography of dry hobbing machine tool. Though the thermography was taken in dark environment to improve the measurement accuracy, the difference of emissivity of different materials still leads to the temperature measurement error. Thus, thermography analysis was oriented toward qualitative analysis to show the characteristics of temperature field of dry hobbing machine tool under the condition that processes with optimization and without optimization. Thermal resistances, whose uncertainty of measurement is 0.2 °C, were calibrated based on international primary standards of measurement.

When the dry hobbing machine tool was processed without optimization, the temperature of measurement points rises with fluctuation. As shown in Fig. 14, *T*#1 ranges from 21.0 to 22.5 °C, *T*#2 ranges from 21.5 to 31.9 °C, *T*#3 ranges from 21.8 to 27.4 °C, and *T*#4 ranges from 23.3 to 35.1 °C. Infrared camera was used to obtain the thermography of dry hobbing machine tool, as shown in Fig. 15. The thermography, which is taken when the dry hobbing machine tool is running about 168 min, shows the temperature gradient of dry hobbing machine tool components.

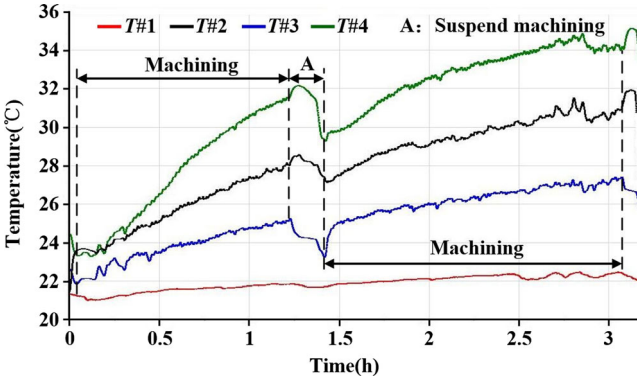

Fig. 14 Temperature of validation points without optimization

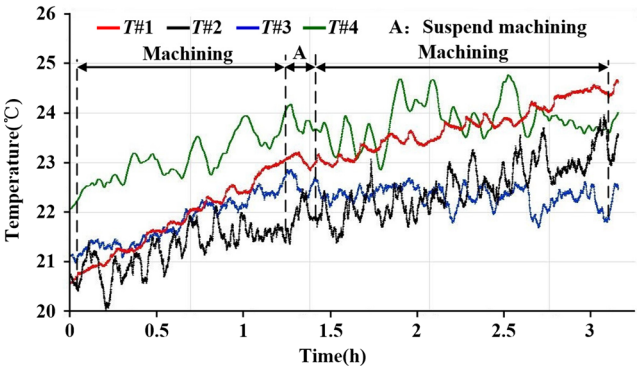

Fig. 16 Temperature of validation points with optimization

Figure 16 shows the temperature of measurement points during the processing with optimization. The fluctuation range of *T*#2 is 4.0 °C, the fluctuation range of *T*#3 is 2.0 °C, and the fluctuation range of *T*#4 is 2.1 °C. The temperature difference between the beginning and the end of *T*#2, *T*#3, and *T*#4 is 2.2, 1.0, and 1.4 °C, respectively. With optimization, the temperature variation of those points is fluctuated in an acceptable range. The thermography, which is shown in Fig. 17, is taken when the dry hobbing machine tool is running about 168 min. The result shows that, with optimization, temperature of components that are close to the cutting zone is lower than without optimization. Furthermore, temperature of other components and interior space air is fluctuated in an acceptable range.

Periodic optimization and heat conduction lead to temperature fluctuation of measurement points. Thus, the temperature data, which fluctuates in a small range, illustrates that the thermal energy control model and the optimization method are effective. However, the temperature data is hard to be a criterion to judge whether the optimization could meet production requirements. The value of accumulated thermal energy is hard to measure. Furthermore, the thermal energy control model, which is used to calculate the thermal energy that accumulated in dry hobbing machine tool, is beneficial to decrease thermal deformation errors in industrial application. Consequently, thermal deformation errors of the dry hobbing machine tool, δ_M, are presented to evaluate whether the optimization could meet production requirements. δ_M, which is the variation of distance between centers of the hob spindle and workpiece spindle in *x* direction, is measured during process. Figure 18 shows the thermal deformation errors with optimization and without optimization. Without optimization, the maximum thermal deformation error is −29.1 μm. That means sampling inspection of workpiece and adjustment is needed in industrial production, which would decrease the production efficiency. With optimization, the thermal deformation errors range from −7 to 3 μm, which is within the tolerance.

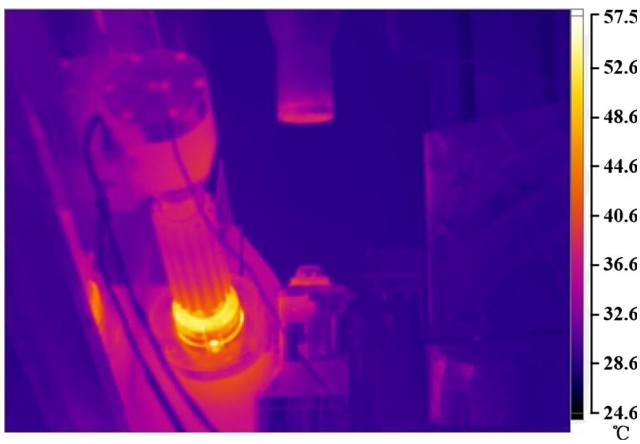

Fig. 15 Thermography of dry hobbing machine tool without optimization

6 Conclusions and outlook

In this paper, a multi-variable driving thermal energy control model of dry hobbing machine tool has been developed. New structures of dry hobbing machine tool, such as air extraction and filtration device, air-cooling component, and magnetic chip conveyor, which would affect the thermal energy accumulation were analyzed. The proposed model shows the

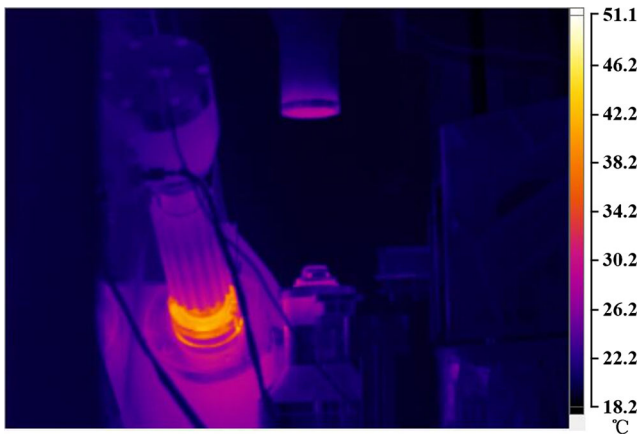

Fig. 17 Thermography of dry hobbing machine tool with optimization

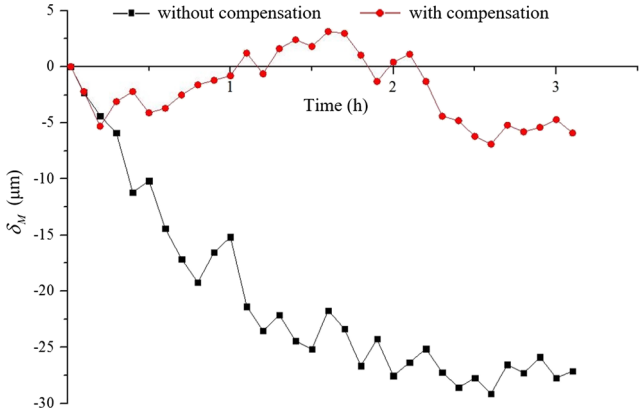

Fig. 18 Thermal deformation errors of dry hobbing machine tool with optimization and without optimization

factors and variables that influence the thermal energy accumulation of dry hobbing machine tool. It provides a method to reduce the thermal energy accumulation by optimizing control variables. With application of the system and the model, the temperature variation and the thermal deformation error variation of dry hobbing machine tool components are fluctuated in an acceptable range, which illustrates that the system and the model are available.

Some kinds of energy change that are caused by hydraulic parts, lighting parts, etc., which have little influence on the thermal energy accumulation of dry hobbing machine tool, are neglected. The thermal energy control model could also be used for cooling device selection under the circumstance that the kind of workpiece is changed, processing parameters are changed, or a new type of dry hobbing machine tool is developed. In this paper, the multi-objective optimization algorithm is a kind of typical example for implementing the multi-variable thermal energy control model. The decision that which kind of optimization algorithm is suitable is affected by complex industrial condition. In summary, to further improve the optimization algorithm, the accuracy of thermal energy control model will be part of future work.

Acknowledgements This research is supported by the National Natural Science Foundation of China (Grant No. 51475058), Chang Jiang Scholars Program of China (Grant No. Q2015150).

References

1. Bryan J (1990) International status of thermal error research. CIRP Ann Manuf Technol 39(2):645–656. doi:10.1016/S0007-8506(07)63001-7
2. Holkup T, Cao H, Kolář P, Altintas Y, Zelený J (2010) Thermo-mechanical model of spindles. CIRP Ann Manuf Technol 59(1):365–368. doi:10.1016/j.cirp.2010.03.021
3. Kim J, Jeong YH, Cho D (2004) Thermal behavior of a machine tool equipped with linear motors. Int J Mach Tools Manuf 44(7):749–758. doi:10.1016/j.ijmachtools.2004.02.006
4. Huang J, Zhou Z, Liu M, Zhang E, Chen M, Pham D, Ji C (2015) Real-time measurement of temperature field in heavy-duty machine tools using fiber bragg grating sensors and analysis of thermal shift errors. Mechatronics 31:16–21. doi:10.1016/j.mechatronics.2015.04.004
5. Abele E, Sielaff T, Schiffler A, Rothenbücher S (2011) Analyzing energy consumption of machine tool spindle units and identification of potential for improvements of efficiency. (pp. 280–285). Berlin, Heidelberg: Springer Berlin Heidelberg. doi:10.1007/978-3-642-19692-8_49
6. Abele E, Altintas Y, Brecher C (2010) Machine tool spindle units. CIRP Ann Manuf Technol 59(2):781–802. doi:10.1016/j.cirp.2010.05.002
7. Li Y, Zhao W, Wu W, Lu B, Chen Y (2014) Thermal error modeling of the spindle based on multiple variables for the precision machine tool. Int J Adv Manuf Technol 72(9):1415–1427. doi:10.1007/s00170-014-5744-4
8. Sarhan AAD (2014) Investigate the spindle errors motions from thermal change for high-precision CNC machining capability. Int J Adv Manuf Technol 70(5):957–963. doi:10.1007/s00170-013-5339-5
9. Züst S, Gontarz A, Pavliček F, Mayr J, Wegener K (2015) Model based prediction approach for internal machine tool heat sources on the level of subsystems. Procedia CIRP 28:28–33. doi:10.1016/j.procir.2015.04.006
10. Bossmanns B, Tu JF (1999) A thermal model for high speed motorized spindles. Int J Mach Tools Manuf 39(9):1345–1366. doi:10.1016/S0890-6955(99)00005-X
11. Sreejith PS, Ngoi BKA (2000) Dry machining: machining of the future. J Mater Process Technol 101(1):287–291. doi:10.1016/S0924-0136(00)00445-3
12. Cao H, Zhu L, Li X, Chen P, Chen Y (2016) Thermal error compensation of dry hobbing machine tool considering workpiece thermal deformation. Int J Adv Manuf Technol 86(5):1739–1751. doi:10.1007/s00170-015-8314-5
13. Weinert K, Inasaki I, Sutherland JW, Wakabayashi T (2004) Dry machining and minimum quantity lubrication. CIRP Ann Manuf Technol 53(2):511–537. doi:10.1016/S0007-8506(07)60027-4
14. Schindler S, Zimmermann M, Aurich JC, Steinmann P (2014) Thermo-elastic deformations of the workpiece when dry turning aluminum alloys—a finite element model to predict thermal effects in the workpiece. CIRP J Mech Sci Technol 7(3):233–245. doi:10.1016/j.cirpj.2014.04.006
15. Han J, Wang L, Wang H, Cheng N (2012) A new thermal error modeling method for CNC machine tools. Int J Adv Manuf Technol 62(1):205–212. doi:10.1007/s00170-011-3796-2
16. Wu CW, Tang CH, Chang CF, Shiao YS (2012) Thermal error compensation method for machine center. Int J Adv Manuf Technol 59(5):681–689. doi:10.1007/s00170-011-3533-x
17. Friderikos O, Maliaris G, David CN, Tsiafis I (2011) An investigation of cutting edge failure due to chip crush in carbide dry hobbing using the finite element method. Int J Adv Manuf Technol 57(1):297–306. doi:10.1007/s00170-011-3298-2
18. Claudin C, Rech J (2009) Development of a new rapid characterization method of hob's wear resistance in gear manufacturing—application to the evaluation of various cutting edge preparations in high speed dry gear hobbing. J Mater Process Technol 209(11):5152–5160. doi:10.1016/j.jmatprotec.2009.02.014
19. Incropera FP, DeWitt DP, Bergman TL, Lavine AS (2007) Fundamentals of heat and mass transfer, 6th edn. J. Wiley, New York
20. Dogu Y, Aslan E, Camuscu N (2006) A numerical model to determine temperature distribution in orthogonal metal cutting. J Mater Process Technol 171(1):1–9. doi:10.1016/j.jmatprotec.2005.05.019

21. Fratila D (2009) Evaluation of near-dry machining effects on gear milling process efficiency. J Clean Prod 17(9):839–845. doi:10.1016/j.jclepro.2008.12.010
22. Chen X, Liu J, He Y, Zhang P, Shan W (2013) Thermal properties of high speed motorized spindle and their effects. Jixie Gongcheng Xuebao/J Mech Eng 49(11):135–142. doi:10.3901/JME.2013.11.135
23. Kauschinger B, Schroeder S (2016) Uncertainties in heat loss models of rolling bearings of machine tools. Procedia CIRP 46:107–110. doi:10.1016/j.procir.2016.03.168
24. Shi H, Ma C, Yang J, Zhao L, Mei X, Gong G (2015) Investigation into effect of thermal expansion on thermally induced error of ball screw feed drive system of precision machine tools. Int J Mach Tools Manuf 97:60–71. doi:10.1016/j.ijmachtools.2015.07.003
25. Koffel G, Ville F, Changenet C, Velex P (2009) Investigations on the power losses in gear transmissions. ARCHIVE Proceedings of the Institution of Mechanical Engineers Part J Journal of Engineering Tribology 1994–1996 (vols 208–210) 223(3):469–479
26. Chen Y, Cao H, Li X, Chen P (2016) The model of spatial forming with multi-cutting-edge for cylindrical gear hobbing and its application. Jixie Gongcheng Xuebao/J Mech Eng 52(9):176–183. doi:10.3901/JME.2016.09.176
27. Dimitriou V, Antoniadis A (2009) CAD-based simulation of the hobbing process for the manufacturing of spur and helical gears. Int J Adv Manuf Technol 41(3):347–357. doi:10.1007/s00170-008-1465-x
28. Vargaftik NB, Touloukian YS (1975) Tables on the thermophysical properties of liquids and gases: in normal and dissociated states, 2nd edn. John Wiley & sons,inc, New york
29. Library WE (1979) American society of heating, refrigerating and air-conditioning engineers. Int J Refrig 2(3):56–57
30. Lemmon EW, Huber ML, Mclinden MO (2010) Nist standard reference database 23: reference fluid thermodynamic and transport properties-refprop. 9.0
31. Thiede S, Herrmann C, Kara S (2011) State of research and an innovative approach for simulating energy flows of manufacturing systems. Glocalized Solutions for Sustainability in Manufacturing—Proceedings of the 18th CIRP International Conference on Life Cycle Engineering 335–340. doi:10.1007/978-3-642-19692-8-58